Report

A comprehensive framework for seasonal controls of leaf abscission and productivity in evergreen broadleaved tropical and subtropical forests

Xueqin Yang,[1,2] Jianping Wu,[2,14] Xiuzhi Chen,[1,*] Philippe Ciais,[3] Fabienne Maignan,[3] Wenping Yuan,[1] Shilong Piao,[4] Song Yang,[1] Fanxi Gong,[1,2,5] Yongxian Su,[2,*] Yuhang Dai,[1,2,6] Liyang Liu,[1,2,3] Haicheng Zhang,[7] Damien Bonal,[8] Hui Liu,[9] Guixing Chen,[1] Haibo Lu,[1] Shengbiao Wu,[10] Lei Fan,[11] Pierre Gentine,[12] and S. Joseph Wright[13]

*Correspondence: chenxzh73@mail.sysu.edu.cn (X.C.); suyongxian@gdas.ac.cn (Y.S.)

Received: February 26, 2021; Accepted: August 18, 2021; Published Online: August 20, 2021; https://doi.org/10.1016/j.xinn.2021.100154

© 2021 The Author(s). This is an open access article under the CC BY-NC-ND license (http://creativecommons.org/licenses/by-nc-nd/4.0/).

Graphical abstract

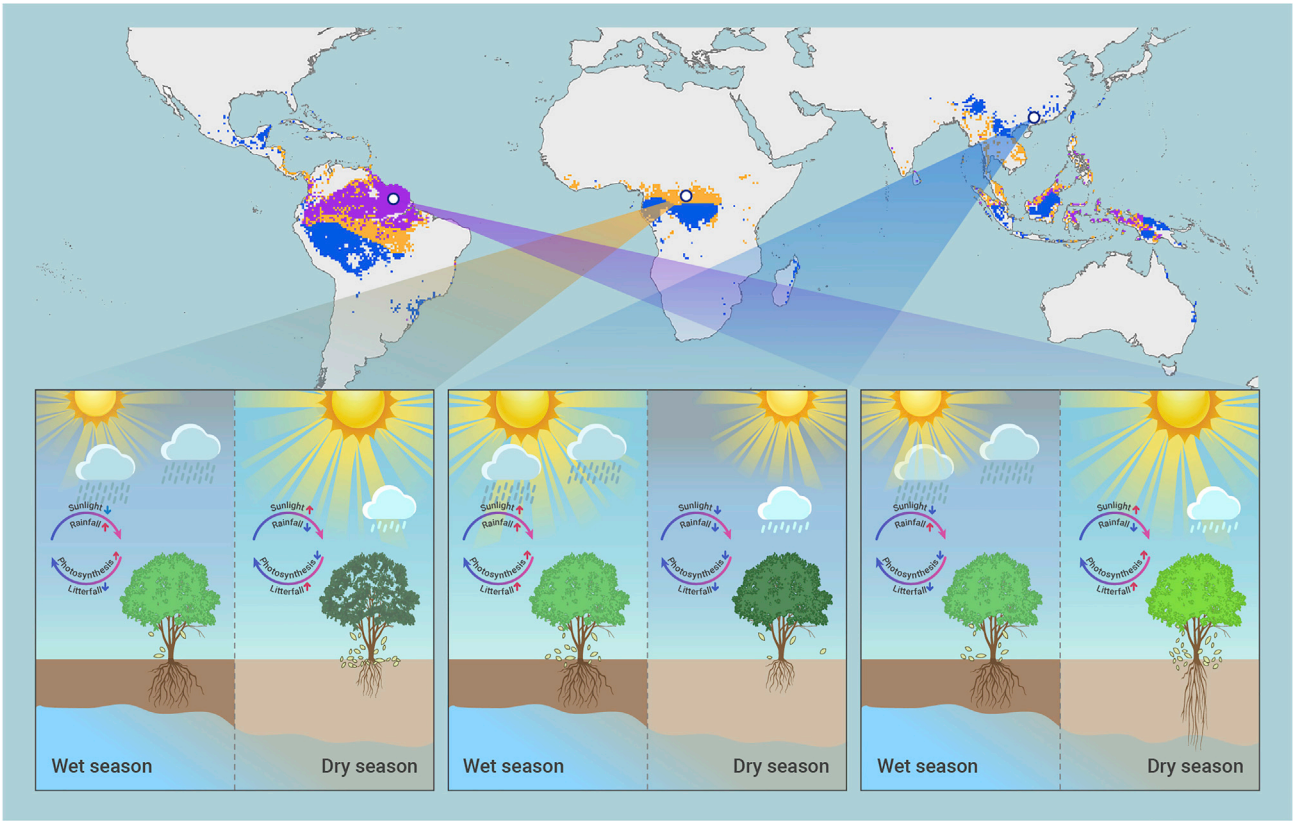

Public summary

- Three climate-phenology regimes are identified across tropical and subtropical forest biomes
- Where light and water limit plant in dry season, litterfall and productivity peak in sunny wet season
- Where light or water alternately limits plant, productivity peaks in wet season with low litterfall
- Where water does not limit plant, litterfall and productivity peak in sunny dry season

Report

A comprehensive framework for seasonal controls of leaf abscission and productivity in evergreen broadleaved tropical and subtropical forests

Xueqin Yang,[1,2] Jianping Wu,[2,14] Xiuzhi Chen,[1,*] Philippe Ciais,[3] Fabienne Maignan,[3] Wenping Yuan,[1] Shilong Piao,[4] Song Yang,[1] Fanxi Gong,[1,2,5] Yongxian Su,[2,*] Yuhang Dai,[1,2,6] Liyang Liu,[1,2,3] Haicheng Zhang,[7] Damien Bonal,[8] Hui Liu,[9] Guixing Chen,[1] Haibo Lu,[1] Shengbiao Wu,[10] Lei Fan,[11] Pierre Gentine,[12] and S. Joseph Wright[13]

[1]Guangdong Province Key Laboratory for Climate Change and Natural Disaster Studies, School of Atmospheric Sciences, Sun Yat-sen University & Southern Marine Science and Engineering Guangdong Laboratory (Zhuhai), Zhuhai 519082, China

[2]Key Lab of Guangdong for Utilization of Remote Sensing and Geographical Information System, Guangdong Open Laboratory of Geospatial Information Technology and Application, Guangzhou Institute of Geography, Guangdong Academy of Sciences, Guangzhou 510070, China

[3]Laboratoire des Sciences du Climat et de l'Environnement, IPSL, CEA-CNRS-UVSQ, Université Paris-Saclay, 91191 Gif sur Yvette, France

[4]Sino-French Institute for Earth System Science, College of Urban and Environmental Sciences, Peking University, Beijing 100871, China

[5]College of Earth Sciences, Chengdu University of Technology, Chengdu 610000, China

[6]College of Forestry and Landscape Architecture, South China Agricultural University, Guangzhou 510000, China

[7]Department of Geoscience, Environment & Society, Université Libre de Bruxelles, Bruxelles, Belgium

[8]INRA, UMR " Ecologie et Ecophysiologie Forestières", Université de Lorraine-INRA, 54280 Champenoux, France

[9]South China Botanical Garden, Chinese Academy of Sciences, Guangzhou 510650, China

[10]School of Biological Sciences, The University of Hong Kong, Pokfulam, Hong Kong

[11]Chongqing Jinfo Mountain Karst Ecosystem National Observation and Research Station, School of Geographical Sciences, Southwest University, Chongqing 400715, China

[12]Department of Earth & Environmental Engineering, Columbia University, New York, NY 10027, USA

[13]Smithsonian Tropical Research Institute, Apartado 0843-03092, Balboa, Panama

[14]These authors contributed equally

*Correspondence: chenxzh73@mail.sysu.edu.cn (X.C.); suyongxian@gdas.ac.cn (Y.S.)

Received: February 26, 2021; Accepted: August 18, 2021; Published Online: August 20, 2021; https://doi.org/10.1016/j.xinn.2021.100154

© 2021 The Author(s). This is an open access article under the CC BY-NC-ND license (http://creativecommons.org/licenses/by-nc-nd/4.0/).

Citation: Yang X., Wu J., Chen X., et al., (2021). A comprehensive framework for seasonal controls of leaf abscission and productivity in evergreen broadleaved tropical and subtropical forests. The Innovation **2(4)**, 100154.

Relationships among productivity, leaf phenology, and seasonal variation in moisture and light availability are poorly understood for evergreen broadleaved tropical/subtropical forests, which contribute 25% of terrestrial productivity. On the one hand, as moisture availability declines, trees shed leaves to reduce transpiration and the risk of hydraulic failure. On the other hand, increases in light availability promote the replacement of senescent leaves to increase productivity. Here, we provide a comprehensive framework that relates the seasonality of climate, leaf abscission, and leaf productivity across the evergreen broadleaved tropical/subtropical forest biome. The seasonal correlation between rainfall and light availability varies from strongly negative to strongly positive across the tropics and maps onto the seasonal correlation between litterfall mass and productivity for 68 forests. Where rainfall and light covary positively, litterfall and productivity also covary positively and are always greater in the wetter sunnier season. Where rainfall and light covary negatively, litterfall and productivity are always greater in the drier and sunnier season if moisture supplies remain adequate; otherwise productivity is smaller in the drier sunnier season. This framework will improve the representation of tropical/subtropical forests in Earth system models and suggests how phenology and productivity will change as climate change alters the seasonality of cloud cover and rainfall across tropical/subtropical forests.

Keywords: tropical forest; leaf abscission and productivity; plant adaptive strategy; climate and phenology regime; climatic driver

INTRODUCTION

Evergreen broadleaved tropical/subtropical forests provide the largest share of global photosynthesis,[1,2] with generally favorable temperatures year round. Despite a perennial canopy, leaves are continuously shed and rejuvenated, and litterfall and photosynthesis peaks occur in different seasons across sites.[1,3,4] Many evergreen broadleaved tropical/subtropical forests experience seasonal constraints of moisture and light availability during recurrent dry and wet seasons.[5–7] These forests exhibit complex leaf shedding and rejuvenation strategies in response to moisture and light availability, and these strategies depend on soil water, atmospheric vapor pressure deficit, and incoming solar radiation. Leaf shedding in the dry season may be an adaptive response to soil water deficits[8–10] or atmospheric aridity.[11–14] Alternatively, leaf shedding in non-water-limited conditions may constitute an adaptive strategy to replace senescent leaves with efficient young leaves to maximize photosynthesis.[5,7,15–17] It remains uncertain where these alternative strategies are important across the evergreen broadleaved tropical/subtropical forests.

In this paper, we propose three qualitative climate-phenology regimes to describe how leaf phenology and forest productivity respond to seasonal climate variation across evergreen broadleaved tropical/subtropical forests. To characterize seasonal climatic variation, we calculate the Pearson correlation coefficient ($R_{climate}$) between mean monthly values of precipitation (Pre) and incoming shortwave radiation (SW) (Figures 1 and S1). We refer to synchronous climates where Pre and SW covary positively ($R_{climate} > 0$) and asynchronous climates where Pre and SW covary negatively ($R_{climate} < 0$). To characterize seasonal variation in plant responses, we calculate the Pearson correlation coefficient ($R_{phenology}$) between monthly litterfall mass and solar-induced fluorescence (SIF) for 68 tropical and subtropical forests (Table S1 and Figure 1; see supplemental methods). Leaves dominate litterfall mass,[18] and the seasonal timing of leaf fall might presage reductions in leaf area to avoid a stressful season or replacement of senescent leaves to capitalize on a favorable season. SIF is a proxy for photosynthetic activity and productivity.[19,20] We validate the photosynthetic proxy using two satellite-based sources for SIF,[21,22] the enhanced vegetation index

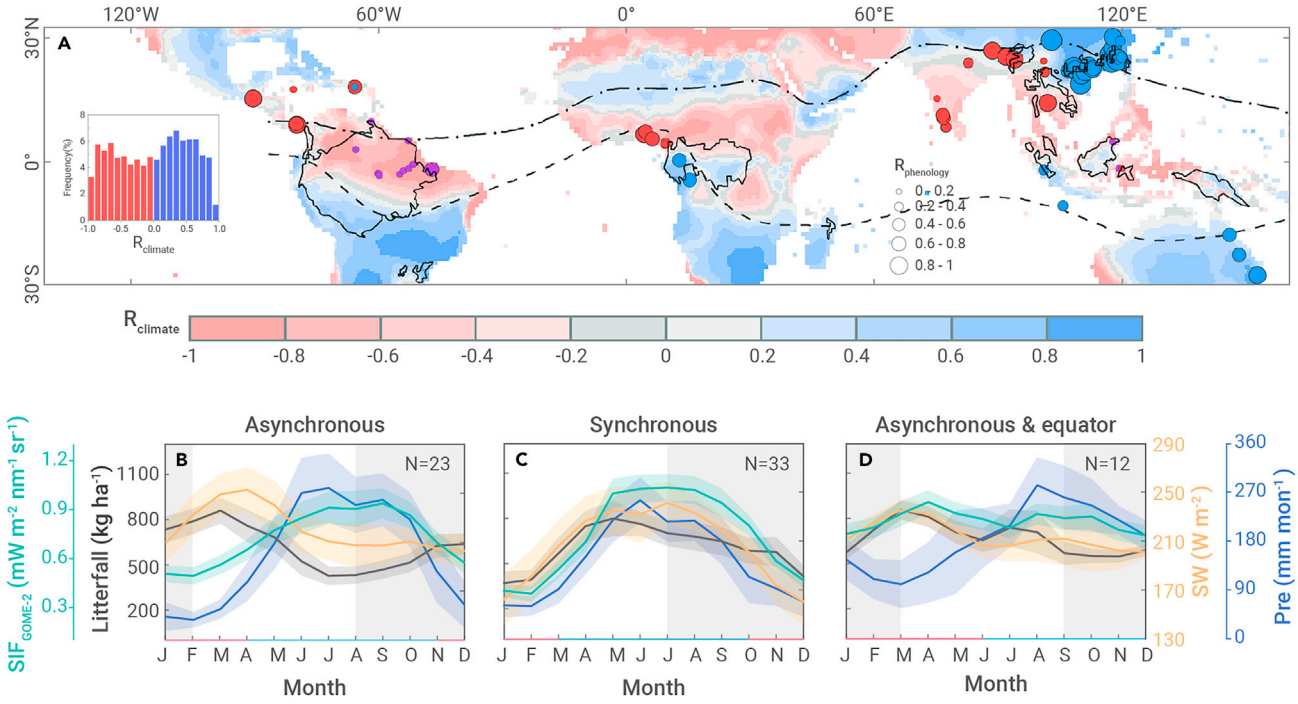

Figure 1. Map of 68 evergreen, broadleaved tropical forests with monthly litterfall (A) Background colors represent the Pearson correlation coefficients ($R_{climate}$) between monthly precipitation (Pre) and incoming shortwave radiation (SW). Symbols represent the Pearson correlation coefficients ($R_{phenology}$) between monthly litterfall and solar-induced fluorescence (SIF) from the National Aeronautics and Space Administration Global Ozone Monitoring Experiment-2 (GOME-2) (SIF_{GOME-2}), a remotely sensed proxy for stand-level photosynthesis. Symbol size represents absolute $R_{phenology}$ values (see inset legend). Symbol color distinguishes positive (blue) and negative (red/purple) $R_{phenology}$. The inset histogram presents $R_{climate}$ for extant evergreen broadleaved tropical forests, which are enclosed by the solid black lines. The dot-dashed and dashed lines represent the general location of the Intertropical Convergence Zone in July and January, respectively (Yan, 2005). (B–D) The mean (±1 SE) monthly litterfall (black), SIF_{GOME-2} (green), SW (orange), and Pre (blue) for sites represented by red (B), blue (C), and purple (D) symbols in (A). Seasonality is standardized to the northern hemisphere, N is the number of litterfall sites, horizontal axis colors separate representative wet (blue, rainfall ≥100 mm) from dry (red, rainfall <100 mm) months, and the gray background identifies the wet- to dry-season transition months. Figure S1 validates $R_{climate}$. Figures S2 and S3 present the monthly litterfall, SIF, Pre, and SW for each site and the mean values for southern hemisphere sites with southern hemisphere seasonality, respectively.

(EVI),[23] near-infrared vegetation reflectance,[24] evapotranspiration (Table S2 and Figures S2–S4),[25] and field observations from five eddy covariance (EC) tower sites from the FLUXNET2015 dataset[26] to test the robustness of our results (Table S3). Seasonal variation in SIF and remotely sensed independent proxies of productivity are closely related in tropical/subtropical forests (Figures S4A, S4C, and S4E).

We hypothesize that the sign of $R_{phenology}$ can be predicted from the sign of $R_{climate}$ and, where $R_{climate}$ is negative, additional insight into the severity of the dry season. Where $R_{climate}$ is positive, we predict that $R_{phenology}$ will also be positive. We refer to this as a synchronous climate-phenology regime, with senescent leaves replaced to maximize productivity in the wetter sunnier season. Where $R_{climate}$ is negative and dry-season moisture availability limits productivity, we predict $R_{phenology}$ will be negative. We refer to this as an asynchronous climate-phenology regime, with litterfall mass increasing as stand-level leaf area and productivity decrease during the drier sunnier season. Finally, where $R_{climate}$ is negative and dry-season moisture availability supports productivity, we predict $R_{phenology}$ will be positive. For reasons that will become apparent later, we refer to this as an asynchronous equatorial climate-phenology regime, with senescent leaves replaced to maximize productivity in the drier sunnier season.

RESULTS

A climate-phenology correlation framework

$R_{climate}$ varies from strongly negative to strongly positive across the pantropic (Figure 1A, background map) and across extant evergreen broadleaved tropical/subtropical forests (Figure 1A, inset histogram). The seasonal movements of the intertropical convergence zone (ITCZ) bring cloudy wet seasons, sunny dry seasons, and negative $R_{climate}$ to a large portion of the tropics.[27,28] Regional features including monsoonal regimes, orography, continentality, and moisture recycling can decouple the regions of rainfall and reduced sunlight[29] and give rise to positive $R_{climate}$. Generally, $R_{climate}$ is positive over parts of equatorial Africa and equatorial Southeast Asia and in areas beyond the reach of the seasonal movements of the ITCZ in the monsoonal regions of southwestern Amazonia, Australia, and the subtropics (Figures 1A and S1). $R_{climate}$ distinguishes the regions where moisture and light potentially limit the plants in the same season (positive $R_{climate}$, Figure 1C) from the regions where moisture and light potentially limit the plants in different seasons (negative $R_{climate}$, Figure 1B). We refer to these as synchronous and asynchronous climates, respectively.

$R_{phenology}$ also varies widely from strongly negative to strongly positive among evergreen broadleaved tropical/subtropical forests and is constrained by $R_{climate}$ when calculated for all 12 months (Figures 1A and 2A). The 12-month $R_{climate}$ and $R_{phenology}$ have the same sign for 63 of the 68 evergreen broadleaved tropical/subtropical forests with litterfall data (exact binomial test, $p < 10^{-13}$). Although we had not anticipated this result, there is also a striking correlation between the absolute values of $R_{climate}$ and $R_{phenology}$ ($r = 0.77$, $p < 10^{-14}$). The relationship between $R_{climate}$ and $R_{phenology}$ is quantitatively as well as qualitatively strong (Figure 2A). Thirty of the 35 forests with negative $R_{climate}$ also have negative $R_{phenology}$ (Figure 2A). In addition, all 33 forests with positive $R_{climate}$ also have positive $R_{phenology}$. We refer to this as the synchronous climate-phenology regime, with litterfall and SIF increasing synchronously with Pre and SW in the wet season (Figure 1C). We infer that these forests exchange leaves, abscising old leaves, thereby increasing litterfall mass and producing new leaves as SW, Pre, and SIF increase.

To further explore the relationship between $R_{climate}$ and $R_{phenology}$, we recalculated $R_{climate}$ and $R_{phenology}$ for the six months that include the wet- to dry-season transition. For the 33 forests in the synchronous climate-phenology regime, $R_{climate}$ and $R_{phenology}$ remained positive (Figures 2A and 2B). In contrast, for seven of the 35 forests with negative $R_{climate}$, the sign of

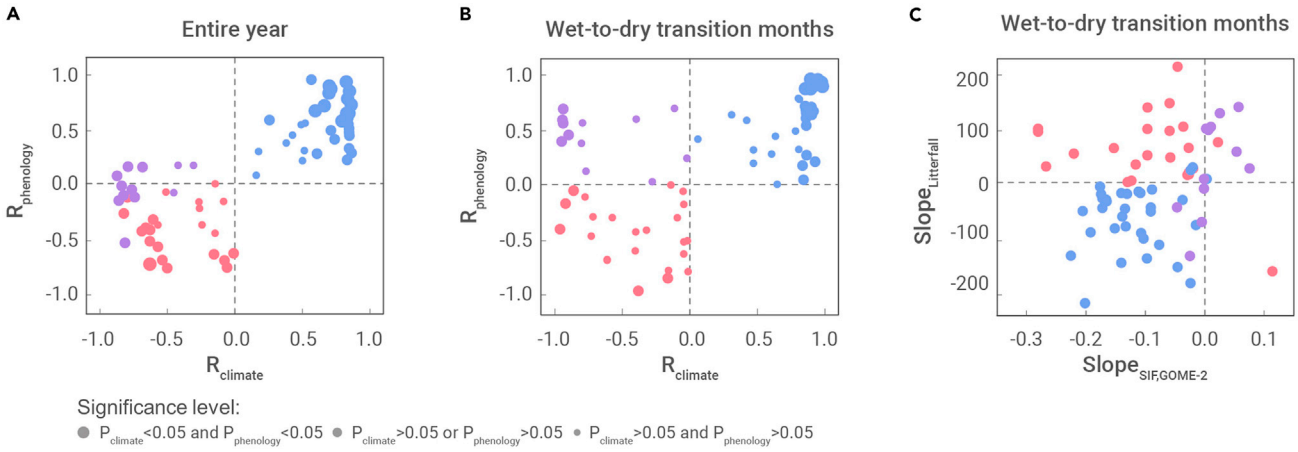

Figure 2. Significance level Scatterplots between $R_{climate}$, the Pearson correlation coefficients between monthly precipitation (Pre) and incoming shortwave radiation (SW), and $R_{phenology}$, the Pearson correlation coefficients between monthly litterfall and SIF_{GOME-2} for the entire year (A) and for six wet- to dry-season transition months (B); and scatterplots between $Slope_{litterfall}$, slopes calculated using litterfall versus month ($Slope_{litterfall}$), and $Slope_{SIF,\ GOME-2}$, slopes calculated using SIF_{GOME-2} versus month, for six wet- to dry-season transition months (C). Symbols represent the 68 litterfall sites with colors as in Figure 1A. The three symbol sizes in plots (A) and (B) represent combinations of significant and insignificant p values for $R_{climate}$ and $R_{phenology}$ ($P_{climate}$ and $P_{phenology}$, respectively; see legend). Representative wet-to-dry transition months for each site are identified by their mean monthly Pre in Data S1.

$R_{phenology}$ changed from negative for 12 months to positive for the six transitional months (Figures 2A and 2B). Twelve of the 35 forests with asynchronous climates ($R_{climate} < 0$) have positive $R_{phenology}$ for the six transitional months (Figure 2B). These 12 forests are in equatorial South America and Southeast Asia (Figure 1A). We refer to this as the asynchronous equatorial climate-phenology regime, with SW, SIF, and litterfall increasing as Pre decreases. The 23 remaining forests with asynchronous climates ($R_{climate} < 0$) also have negative $R_{phenology}$. We refer to this as the asynchronous climate-phenology regime, with SW and litterfall increasing and SIF decreasing as Pre decreases.

The slope of the relationships between month and litterfall and SIF ($Slope_{litterfall}$ and $Slope_{SIF}$, respectively) for the 6-month transition from wet to dry season is broadly consistent with this interpretation (Figure 2C). From the late wet into early dry season, litterfall mass and SIF tend to decline for the synchronous climate-phenology regime (blue symbols in Figure 2C), litterfall mass tends to increase and SIF tends to decline for the asynchronous climate-phenology regime (red symbols in Figure 2C), and litterfall mass tends to increase while SIF increases or holds steady for the asynchronous equatorial climate-phenology regime (purple symbols in Figure 2C). These temporal trends confirm the direction of plant responses entering the dry season for each climate-phenology regime.

Importantly, the p-value analyses show that the bigger the values of $R_{climate}$ and $R_{phenology}$, the smaller the p value (Figure 2A), implying that a stronger seasonal covariance between sunlight and rainfall ($p < 0.05$) produces a stronger seasonal covariance in leaf flush and shedding processes ($p < 0.05$). The thresholds for a significant $R_{climate}$-$R_{phenology}$ correlation are $R_{climate} \approx 0.5$ and $R_{climate} \approx 0.5$ for the entire year. However, climates with weaker seasonal light-moisture correlations ($p > 0.05$) usually exhibit weaker correlation in leaf phenology ($p > 0.05$), i.e., leaf flush and shedding, which might be greatly influenced by other local factors (such as wind)[30,31] and be more different between plant species.[32,33]

To test the robustness of the $R_{climate}$-$R_{phenology}$ quadrantal space, we applied satellite-based MODIS EVI and $SIF_{TROPOMI}$ from independent sensors as alternatives of SIF_{GOME-2} to recalculate $R_{phenology}$. With these datasets, the $R_{climate}$-$R_{phenology}$ space based on monthly MODIS EVI and monthly litterfall also falls in two quarters, with positive $R_{climate}$ having positive $R_{phenology}$ and negative $R_{climate}$ having negative $R_{phenology}$ (exact binomial test, $p < 10^{-13}$) (Figure S14). These analyses still support that a stronger seasonal sunlight-moisture correlation ($p < 0.05$) produces stronger seasonal correlation in leaf phenology ($p < 0.05$), while a weaker seasonal sunlight-moisture correlation ($p > 0.05$) usually exhibits weaker correlation in leaf phenology ($p > 0.05$). Overall, the $R_{climate}$-$R_{phenology}$ space based on monthly $SIF_{TROPOMI}$ and monthly litterfall shows similar pattern (Figure S15), although the period of $SIF_{TROPOMI}$ time series do not overlap with the litterfall data. Additionally, the monthly tower-based gross primary productivity (GPP) is used as an alternative of remotely sensed photosynthetic proxies to compare with monthly litterfall mass and meteorological observations for five EC flux tower sites in tropical forests from the FLUXNET2015 dataset (Table S3).[26] $R_{phenology}$ is calculated between monthly GPP and monthly litterfall mass. Three Amazonian sites with negative $R_{climate}$ values have negative values of $R_{phenology}$ while two subtropical sites in China with positive $R_{climate}$ also have positive $R_{phenology}$. Analyses from five tropical/subtropical flux tower sites are consistent with the proposed climate-phenology space.

Satellite-derived SIF_{GOME-2} enables generalization to all extant evergreen broadleaved tropical forests and identifies one seasonal phenology wherever $R_{climate}$ is positive and two qualitatively distinct seasonal phenologies wherever $R_{climate}$ is negative. Figure 3 maps the combinations of positive and negative values of $R_{climate}$ and the difference between mean SIF_{GOME-2} for dry and wet months (ΔSIF_{GOME-2}) for extant evergreen broadleaved tropical/subtropical forests. The spatial distribution of ΔEVI and $\Delta SIF_{TROPOMI}$ largely confirms the spatial distribution of ΔSIF_{GOME-2} (cf. Figures S16, S17, and 3A–3C). The combination of positive $R_{climate}$ and positive ΔSIF does not occur. Where seasonal Pre and SW variation is synchronous (positive $R_{climate}$), SIF and productivity always average greater values in wet months than in dry months (blue in Figure 3). This is the synchronous climate-phenology regime identified for the 68 litterfall sites. In contrast, where seasonal Pre and SW variation is asynchronous (negative $R_{climate}$), SIF can take greater values in either wet (yellow in Figure 3) or dry (purple in Figure 3) months. We refer to these as asynchronous and asynchronous equatorial climate-phenology regimes, respectively. The asynchronous equatorial (purple) regime is restricted to equatorial latitudes in the Americas and Asia (Figures 3D and 3F). Twelve forests with litterfall data fall into the asynchronous equatorial regime. Although SIF averages to greater values in dry months than in wet months for all 12 forests, the absolute value of the seasonal difference is small compared with the remaining 56 forests (Figure S6). This limited seasonal variation in SIF constrains the absolute value of $R_{phenology}$ to small values (see purple symbols in Figure 2A). We therefore recalculated $R_{phenology}$ and $R_{climate}$ for the six months that capture plant responses to the critical wet- to dry-season transition. The sign of $R_{climate}$ is unaffected (cf. Figures 2A and 2B) while the sign of $R_{phenology}$ changes for seven sites with negative $R_{climate}$, confirming that there are two qualitatively distinct phenological responses to negative $R_{climate}$ (purple versus red symbols in Figure 2B).

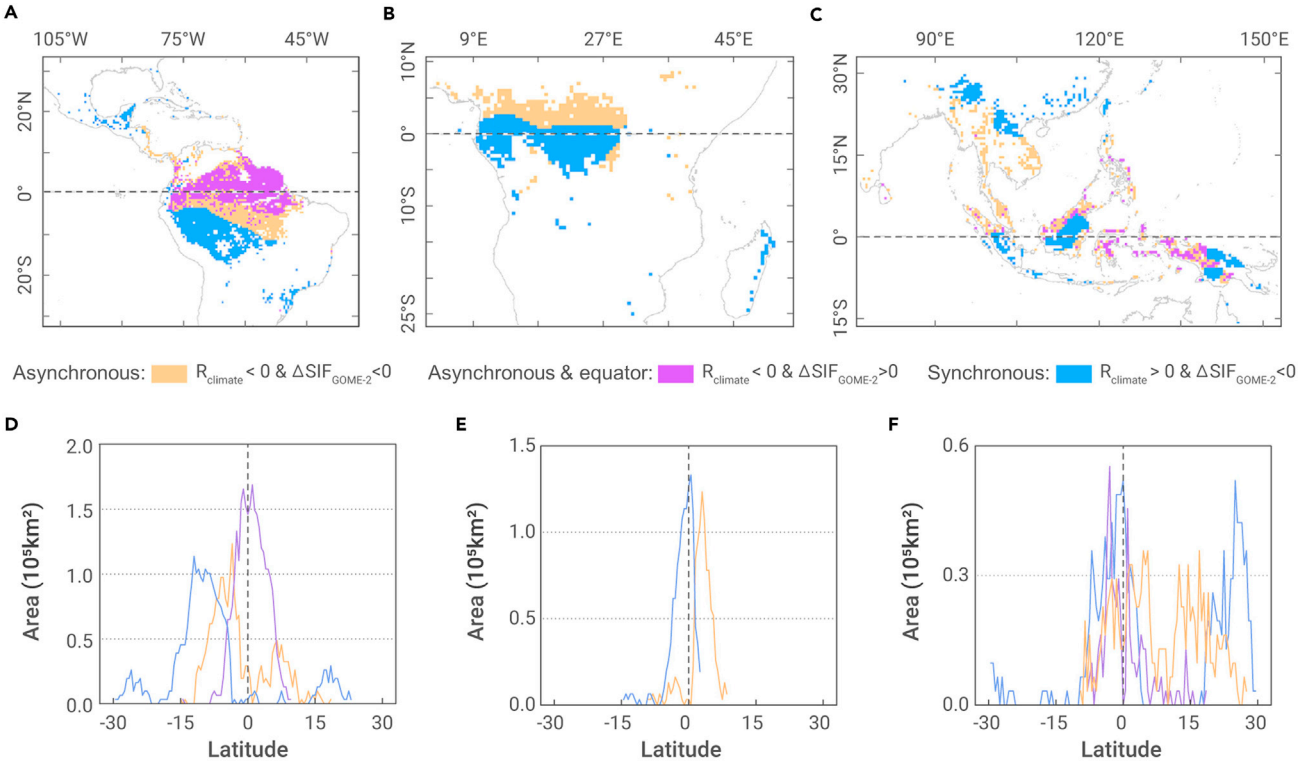

Figure 3. asynchronous regime, synchronous regime, asynchronous equatorial regime Maps of combinations of the sign of $R_{climate}$ and ΔSIF_{GOME-2} and their latitudinal distributions for evergreen broadleaved tropical forests in the Americas (A and D), Africa (B and E), and Asia, New Guinea, and Australia (C and F). Blue, yellow, and purple represent the pixels with positive $R_{climate}$ and negative ΔSIF_{GOME-2}, negative $R_{climate}$ and ΔSIF_{GOME-2}, and negative $R_{climate}$ and positive ΔSIF_{GOME-2}, respectively. The fourth possible combination (positive $R_{climate}$ and ΔSIF_{GOME-2}) does not occur for evergreen broadleaved tropical forests. $R_{climate}$ is the Pearson correlation coefficient between the monthly values of precipitation (Pre) and incoming shortwave radiation (SW). SIF_{GOME-2} is solar-induced fluorescence. ΔSIF_{GOME-2} equals the difference in mean SIF_{GOME-2} between dry and wet months (see supplemental methods for definition of dry and wet months). The Australian wet tropics have positive $R_{climate}$ and negative ΔSIF_{GOME-2} and are included in (F) but not (C).

Notably, the MODIS EVI confirms well (89% of total pixels) with the spatial variation in seasonality observed for SIF_{GOME-2} (Figure S16). (The $SIF_{TROPOMI}$ started from April 2018.) The $\Delta SIF_{TROPOMI}$ also shows a spatial pattern similar to that of ΔSIF_{GOME-2} (83% of total pixels) and ΔEVI (82% of total pixels) (Figure S17). However, $\Delta SIF_{TROPOMI}$ shows certain discrepancies with ΔSIF_{GOME-2} and ΔEVI in spatial patterns, and the areas of asynchronous equatorial climate-phenology regime shrink (purple in Figure S17).

Three tropical/subtropical climate-phenology regimes

A straightforward hypothesis is that moisture availability exerts first-order control on the productivity in tropical/subtropical forests.[34] Where dry-season moisture availability is insufficient, leaf abscission peaks in the dry season to reduce the risk of hydraulic failure, and productivity peaks in the wet season. Where moisture availability is adequate year round, light availability controls productivity. Leaf turnover, including leaf abscission and presumably new leaf production, peaks in the sunnier season to replace senescent leaves with new leaves with greater photosynthetic potential, which in turn contributes to greater productivity in the sunnier season. This hypothesis predicts dry-season severity and the direction of temporal trends in litterfall and SIF during the wet-to-dry transition for the three climate-phenology regimes of Figures 2B and 3.

For the asynchronous climate-phenology regime (red in Figure 2 and yellow in Figure 3), we predict strong dry seasons and increasing litterfall and decreasing productivity during the wet-to-dry transition. For the 23 litterfall sites in the asynchronous climate-phenology regime, dry seasons are relatively strong. The maximum cumulative water deficit (MCWD)[35] averages −210 mm throughout the year (Figure S18), and the atmospheric evaporative demand quantified by vapor pressure deficit (VPD) is substantially larger in dry months than in wet months (Figures S4B and S7). Across all regions of broadleaved tropical/subtropical forests characterized by the asynchronous climate-phenology regime, the monthly MCWD is −134 mm on average annually, and VPD averages substantially larger values in dry months than in wet months (Figure S10). The predicted increase in litterfall and decrease in SIF during the wet-to-dry transition hold for 21 of 23 sites (Figure 2C; exact binomial test, $p < 10^{-10}$). We infer that strong dry-season atmospheric and soil moisture deficits favor leaf abscission to minimize dry-season transpiration, and that insufficient rainfall dominantly constrains productivity until the wet season returns. This climate-phenology regime was previously hypothesized to prevail over all tropical/subtropical forests.[36] We show that 33% of evergreen broadleaved tropical/subtropical forest areas and 23 of the 68 litterfall sites are characterized by the asynchronous climate-phenology regime (yellow in Figure 3).

For the synchronous climate-phenology regime (blue in Figures 2 and 3), SW is greatest in the wet season (Figures 1C, S9, and S12), and relatively low SW and VPD should ameliorate dry-season conditions enabling leaf retention through the dry season. We predict that litterfall and productivity will increase to peak values as light and moisture availabilities increase during the dry-to-wet transition and then decrease during the wet-to-dry transition. For the 33 litterfall sites in the synchronous climate-phenology regime, dry seasons are indeed surprisingly mild, with monthly MCWD averaging −71 mm throughout the year (Figure S18); however, this does not hold across all regions of broadleaved tropical/subtropical forests characterized by the synchronous climate-phenology regime (Figure S12) because there are relatively severe dry seasons in southeastern Amazonia (Figure S19). The predicted decrease in litterfall and SIF during the wet-to-dry transition holds for 29 of the 33 sites (Figure 2C; binomial test, $p < 10^{-13}$). We infer that the increasing atmospheric water deficits (VPD) (Figure S9) initiate wet-season leaf turnover and that the increasing light levels boost increased productivity during the wet season for the 43% of extant evergreen broadleaved tropical/subtropical forests characterized by the synchronous climate-phenology regime (blue in Figure 3). This

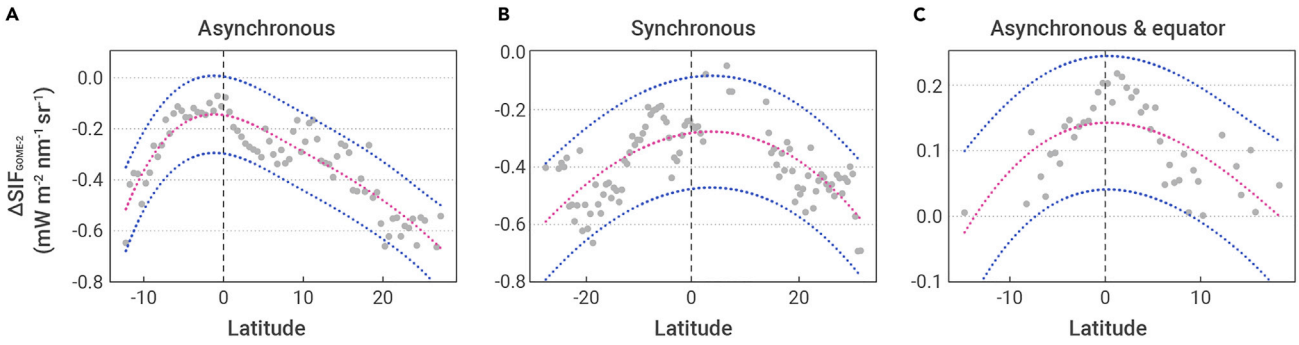

Figure 4. Latitudinal variation in $\Delta SIF_{GOME\text{-}2}$ for the asynchronous (A, yellow in Figure 3), synchronous (B, blue in Figure 3), and asynchronous equatorial (C, purple in Figure 3) regimes. Note the unique vertical scale in (C). Black symbols are mean values for 0.5°-latitude bands. Red lines were fitted using generalized additive models, and blue lines represent the 95% confidence intervals. $SIF_{GOME\text{-}2}$ is solar-induced fluorescence. $\Delta SIF_{GOME\text{-}2}$ equals the difference in mean $SIF_{GOME\text{-}2}$ between dry and wet months (see supplemental methods for definition of dry and wet months).

climate-phenology regime has not been recognized previously. We novelly detect this synchronous climate-phenology regime where the $R_{climate}$ and $R_{phenology}$ are both positive in the proposed $R_{climate}$-$R_{phenology}$ spaces (Figure 2B).

For the asynchronous equatorial climate regime (purple in Figures 2 and 3), we predict increasing litterfall and productivity during the wet-to-dry transition and very slight soil moisture limitation of photosynthesis. Saleska et al.[3] first recognized this climate-phenology regime as a dry-season "green-up" or dry-season leaf production. Here, for the first time, we delineate the regional boundaries of this climate-phenology regime with a large compilation of field and satellite data. Mild dry seasons and/or soil water accessed by deep roots appear to maintain adequate year-round moisture supplies in parts of Amazonia and the Maritime Continent.[34] Where the asynchronous equatorial climate regime prevails, such as in the Maritime Continent and western Amazonia, dry seasons are mild with MCWD close to zero (Figures S8B, S11B, and S11C) while, in eastern Amazonia, deep roots can draw soil water reserves,[34] maintaining moisture supplies during a more severe dry season (Figures S8A and S11A). The predicted increase in litterfall and SIF during the wet-to-dry transition holds for 8 of 12 sites (Figure 2C; binomial test, $p = 0.0028$). We infer that increasing atmospheric drought and decreasing soil moisture availability initiate dry-season leaf turnover, but moisture deficits do not reach levels that constrain leaf production or canopy photosynthesis. The increases in light levels initiate the dry-season "green-up" and productivity growth, which were identified by Saleska et al.,[3] for the 24% of extant evergreen broadleaved tropical/subtropical forests characterized by the asynchronous equatorial climate-phenology regime (purple in Figure 3).

Causes of geographical distributions of three climate-phenology regimes

Continuous climatic and phenological variations underlie our trichotomy of qualitative climate-phenology regimes and together with their latitudinal distributions provide insight into causation, which combines Earth's obliquity and local effects. The Earth's obliquity causes uneven surface heating that drives the seasonal movements of the ITCZ and links the latitudinal position of the ITCZ, longer days, and increased solar inputs.[28] As an example, top-of-atmosphere (TOA) solar radiation is 70% greater for summer than winter solstices at the Tropic of Cancer but just 9% greater for equinoxes than solstices at the equator. Thus, the seasonal increases in TOA radiation at higher latitudes are more likely to outweigh the seasonal reductions in atmospheric transmissivity associated with the cloudy ITCZ and introduce synchronous climates (i.e., positive $R_{climate}$) and the synchronous climate-phenology regime at the higher tropical latitudes. The seasonal movements of the ITCZ are also more likely to introduce asynchronous climates (i.e., negative $R_{climate}$) at the lower tropical latitudes as seasonal variation in TOA radiation declines. The mean position of the ITCZ is close to the equator, and the ITCZ crosses the equator soon after the equinoxes. As a consequence, average annual rainfall is greatest (Figure S20A), the number of dry months is smallest (Figure S20B), moisture availability is least likely to limit productivity, and the difference between mean SIF for dry and wet months ($\Delta SIF_{GOME\text{-}2}$) is greatest at the equator for all three climate-phenology regimes (Figure 4). To summarize, we expect to find the synchronous, asynchronous, and asynchronous equatorial climate-phenology regimes at higher, intermediate, and equatorial tropical latitudes, respectively, due solely to the Earth's obliquity.

Regional effects influence this pattern on each tropical continent. The expected latitudinal distributions are clearest in the Americas, where the synchronous regime is restricted to latitudes poleward of 14°N and 10°S, the asynchronous regime is most frequent between 5° and 15°N and 2°–11°S, and the asynchronous equatorial regime prevails between 9°N and 6°S (Figures 3A and 3D). The most important local effect concerns the limited movement of the ITCZ, which does not reach the Caribbean islands or southwestern Amazonia where synchronous climates extend to 2°S (Figure 1A). The expected latitudinal distributions are also evident in Asia/Australia, where the synchronous regime predominates poleward of 19°N and 15°S and the asynchronous regime predominates between 10° and 15°N. The most important local effect concerns the limited rainfall seasonality and the resulting mix of all three climate-phenology regimes across the equatorial Maritime Continent (Figures 3C and 3F).[37] The expected latitudinal distribution breaks down in equatorial West Africa, dominated by a monsoonal climate,[29,38] where mean annual rainfall and the short duration of the wet season are insufficient to maintain dry-season productivity,[34,39,40] bringing the synchronous regime to unusually low latitudes (Figures 3B and 3E).

DISCUSSION

This study shows that three climate-phenology regimes explain the variation in climate and plant responses observed across all humid tropical/subtropical forests. In a cost-benefit framework, adaptive strategies of shedding and producing leaves appear as a response to light and water availability.[41] Trees adapt their leaf phenology to avoid unfavorable environments such as limited light and water, and maximize their growth rate.[42,43] From this perspective, there are two adaptive responses to seasonal variation in moisture and light availability. When plants suffer severe dry-season water stress, dry-season leaf abscission minimizes the costs and avoids hydraulic failure.[44,45] When trees experience adequate moisture availability year round, exchanging old, senescent leaves for new, efficient leaves in the sunnier season maximizes light capture and productivity.[9,10,17,46] The asynchronous and synchronous climate-phenology regimes are consistent with this conceptual cost-benefit framework.

Forests in the asynchronous climate-phenology regime suffer severe water stress in the dry sunny season (Figure S21). Insufficient soil water supplies and high VPD tend to jointly enhance the abscisic acid levels in leaves, accelerating leaf senescence and shedding.[45,47–49] Plants abscise old leaves with low photosynthetic capacity, thereby decreasing transpiration and protecting the xylem from embolisms, thus reducing maintenance respiration costs.[44,45,50–53] Nonetheless, light use efficiency (LUE) and water use

Report

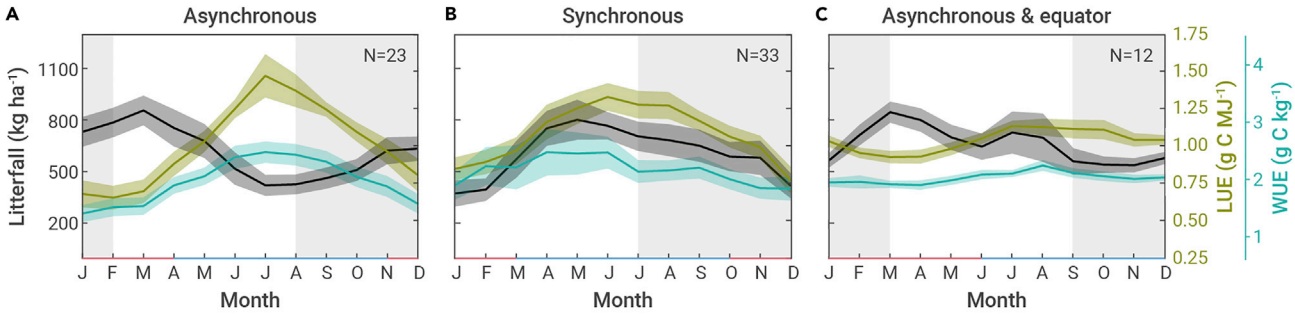

Figure 5. Mean (±1 SE) monthly litterfall (black), light use efficiency (LUE, olive green), and water use efficiency (WUE, light blue) for the sites in asynchronous (A), synchronous (B) and asynchronous equatorial (C) regimes. Horizontal axis colors separate representative dry (red, <100 mm rainfall) and wet (blue, ≥100 mm rainfall) months. The gray background identifies representative late wet and early dry season months. Seasonality is standardized to the northern hemisphere.

efficiency (WUE) both decrease during the dry season (Figure 5A). Our regional correlation analysis shows that more than half of humid tropical/subtropical forests with negative $R_{climate}$ decrease canopy photosynthesis during the dry seasons.

Forests in the synchronous climate-phenology regime experience mild or little seasonal water stress[54–56] and prioritize light acquisition to maximize photosynthesis. In these forests, old leaves are shed while new and more efficient leaves are produced as rainfall and radiation increase in wet seasons.[25,57–59] Both seasonal LUE and seasonal WUE at ecosystem level increase during the sunnier wet season (see supplemental methods and Figure 5B). This leaf phenology strategy benefits from presenting young leaves with high LUE when light availability is greatest.[6,15] To optimize resources for maximizing light use, plant may translocate foliar nutrients from old leaves to new leaves, which may accelerate the abscission of old leaves.[60–63]

The adaptive strategies of leaf flush and leaf shedding are more complex under the asynchronous equatorial climate regime. Plant responses to the asynchronous equatorial climate regime include leaf shedding in the early dry season followed closely by increases in photosynthesis in the later dry season in Amazonian forests.[63–65] Amazonian studies disagree on whether old leaves are shed in response to water stress[9,10] or whether old leaves are shed while water supplies are adequate.[7,12,63] In either case, with the canopy rejuvenated with efficient young leaves, Amazonian forests characterized by the asynchronous equatorial climate regime maintain transpiration and canopy photosynthesis during the sunny dry season.[66,67] Our results show that LUE and WUE are relatively constant year round with a slight peak at the start of the dry season (Figure 5C).

Conclusion

Our framework advances the understanding of the control of leaf phenology and productivity in three ways for evergreen broadleaved tropical/subtropical forests. First, two qualitatively distinct climate regimes with light and moisture potentially limiting plants in the same season or in different seasons prevail over 43% and 57% of the extant evergreen broadleaved tropical/subtropical forest, respectively (Figure 1A). Second, a single phenological response occurs wherever light and moisture potentially limit the plant phenology in the same season, with peak litterfall and productivity in the sunnier wetter season (Figure 1C). We also confirm two phenological responses where light and moisture potentially limit the plant phenology in different seasons, with productivity tracking light availability where moisture supplies permit and with moisture availability elsewhere. Third, the ITCZ and regional climate drivers mostly explain the geographic distributions of the three climate-phenology regimes. This framework will improve the representation of leaf phenology and the seasonal controls of productivity in evergreen broadleaved tropical/subtropical forests in Earth system models,[5,68] has implications for the reproductive phenology of tropical/subtropical forest plants,[15,69] and suggests how leaf phenology and productivity will change as climate change alters the seasonality of cloud cover, atmospheric transmissivity, and rainfall across tropical/subtropical forests.

REFERENCES

1. Sayer, E.J., Heard, M.S., Grant, H.K., et al. (2011). Soil carbon release enhanced by increased tropical forest litterfall. Nat. Clim. Change ***1***, 304–307.
2. Giardina, F., Konings, A.G., Kennedy, D., et al. (2018). Tall Amazonian forests are less sensitive to precipitation variability. Nat. Geosci. ***11***, 405–409.
3. Saleska, S.R., Miller, S.D., Matross, D.M., et al. (2003). Carbon in Amazon forests: unexpected seasonal fluxes and disturbance-induced losses. Science ***302***, 1554–1557.
4. Leff, J.W., Wieder, W.R., Taylor, P.G., et al. (2012). Experimental litterfall manipulation drives large and rapid changes in soil carbon cycling in a wet tropical forest. Glob. Change Biol. ***18***, 2969–2979.
5. Chen, X., Maignan, F., Viovy, N., et al. (2020). Novel representation of leaf phenology improves simulation of Amazonian evergreen forest photosynthesis in a land surface model. J. Adv. Model. Earth Sy. ***12***. https://doi.org/10.1029/2018MS001565.
6. De Weirdt, M., Verbeeck, H., Maignan, F., et al. (2012). Seasonal leaf dynamics for tropical evergreen forests in a process-based global ecosystem model. Geosci. Model Dev. ***5***, 1091–1108.
7. Tang, H., and Dubayah, R. (2017). Light-driven growth in Amazon evergreen forests explained by seasonal variations of vertical canopy structure. Proc. Natl. Acad. Sci. USA ***114***, 2640–2644.
8. Asner, G.P., and Alencar, A. (2010). Drought impacts on the Amazon forest: the remote sensing perspective. New Phytol. ***187***, 569–578.
9. Brando, P.M., Goetz, S.J., Baccini, A., et al. (2010). Seasonal and interannual variability of climate and vegetation indices across the Amazon. Proc. Natl. Acad. Sci. USA ***107***, 14685–14690.
10. Davidson, E.A., de Araújo, A.C., Artaxo, P., et al. (2012). The Amazon basin in transition. Nature ***481***, 321–328.
11. Myers, B.A., Williams, R.J., Fordyce, I., et al. (1998). Does irrigation affect leaf phenology in deciduous and evergreen trees of the savannas of northern Australia? Austral. Ecol. ***23***, 329–339.
12. Lee, J.E., Frankenberg, C., van der Tol, C., et al. (2013). Forest productivity and water stress in Amazonia: observations from GOSAT chlorophyll fluorescence. P. Roy. Soc. B-biol. Sci. ***280***, 20130171.
13. Zhang, Y., Xiao, X., Zhou, S., et al. (2016). Canopy and physiological controls of GPP during drought and heat wave. Geophys. Res. Lett. ***43***, 3325–3333.
14. Xu, X., Medvigy, D., Joseph, W.S., et al. (2017). Variations of leaf longevity in tropical moist forests predicted by a trait-driven carbon optimality model. Ecol. Lett. ***20***, 1097–1106.
15. Wright, S.J., and van Schaik, C.P. (1994). Light and the phenology of tropical trees. Am. Nat. ***143***, 192–199.
16. Xiao, X., Zhang, Q., Saleska, S., et al. (2005). Satellite-based modeling of gross primary production in a seasonally moist tropical evergreen forest. Remote Sens. Environ. ***94***, 105–122.
17. Wu, J., Albert, L.P., Lopes, A.P., et al. (2016). Leaf development and demography explain photosynthetic seasonality in Amazon evergreen forests. Science ***351***, 972–976.
18. Chave, J., Navarrete, D., Almeida, S., et al. (2010). Regional and seasonal patterns of litterfall in tropical South America. Biogeosciences ***7***, 43–55.
19. Joiner, J., Guanter, L., Lindstrot, R., et al. (2013). Global monitoring of terrestrial chlorophyll fluorescence from moderate spectral resolution near-infrared satellite measurements: methodology, simulations, and application to GOME-2. Atmos. Meas. Tech. ***6***, 2803–2823.
20. Joiner, J., Yoshida, Y., Guanter, L., et al. (2016). New methods for the retrieval of chlorophyll red fluorescence from hyperspectral satellite instruments: simulations and application to GOME-2 and SCIAMACHY. Atmos. Meas. Tech. ***9***, 3939.
21. Köhler, P., Frankenberg, C., Magney, T.S., et al. (2018). Global retrievals of solar-induced chlorophyll fluorescence with TROPOMI: first results and intersensor comparison to OCO-2. Geophys. Res. Lett. ***45***, 10456–10463.

22. Doughty, R., Köhler, P., Frankenberg, C., et al. (2019). TROPOMI reveals dry-season increase of solar-induced chlorophyll fluorescence in the Amazon forest. Proc. Natl. Acad. Sci. USA ***116***, 22393–22398.
23. Didan, K. (2015). MOD13C2 MODIS/Terra Vegetation Indices Monthly L3 global 0.05Deg CMG V006 [Data Set] (NASA EOSDIS LP DAAC). https://doi.org/10.5067/MODIS/MOD13C2.006.
24. Badgley, G., Field, C.B., and Berry, J.A. (2017). Canopy near-infrared reflectance and terrestrial photosynthesis. Sci. Adv. ***3***, e1602244.
25. Zhang, Q., Manzoni, S., Katul, G., et al. (2014). The hysteretic evapotranspiration—vapor pressure deficit relation. J. Geophys. Res. Biogeosciences ***119***, 125–140.
26. Pastorello, G., Trotta, C., Canfora, E., et al. (2020). The FLUXNET2015 dataset and the ONEFlux processing pipeline for eddy covariance data. Sci. Data ***7***, 225.
27. Ratan, R., and Venugopal, V. (2013). Wet and dry spell characteristics of global tropical rainfall. Water Resour. Res. ***49***, 3830–3841.
28. Ridley, H., Asmerom, Y., Baldini, J., et al. (2015). Aerosol forcing of the position of the intertropical convergence zone since AD 1550. Nat. Geosci. ***8***, 195–200.
29. Nicholson, S.E. (2018). The ITCZ and the seasonal cycle over equatorial Africa. B. Am. Meteorol. Soc. ***99***, 337–348.
30. Lim, A.C.F., Suzuki, M., Ohte, N., et al. (2009). Evapotranspiration patterns for tropical rainforests in southeast Asia: a model performance examination of the Biome-BGC model. Bull. Tokyo Univ. For. ***120***, 29–44.
31. De Queiroz, M.G., da Silva, T.G.F., Zolnier, S., et al. (2019). Seasonal patterns of deposition litterfall in a seasonal dry tropical forest. Agr. For. Meteorol. ***279***, 107712.
32. Gonçalves, J.F., Jr., de Souza Rezende, R., Gregório, R.S., et al. (2014). Relationship between dynamics of litterfall and riparian plant species in a tropical stream. Limnologica ***44***, 40–48.
33. Guo, Y., Chen, H.Y., Mallik, A.U., et al. (2019). Predominance of abiotic drivers in the relationship between species diversity and litterfall production in a tropical karst seasonal rainforest. For. Ecol. Manag. ***449***, 117452.
34. Guan, K., Pan, M., Li, H., et al. (2015). Photosynthetic seasonality of global tropical forests constrained by hydroclimate. Nat. Geosci. ***8***, 284–289.
35. Zemp, D.C., Schleussner, C., Barbosa, H.M., et al. (2017). Self-amplified Amazon forest loss due to vegetation-atmosphere feedbacks. Nat. Commun. ***8***, 14681.
36. Reich, P.B., and Borchert, R. (1984). Water stress and tree phenology in a tropical dry forest in the lowlands of Costa Rica. J. Ecol. ***72***, 61–74.
37. Chang, C.P., Wang, Z., McBride, J., et al. (2005). Annual cycle of Southeast Asia—Maritime Continent rainfall and the asymmetric monsoon transition. J. Clim. ***18***, 287–301.
38. Hartman, A.T. (2020). Tracking mesoscale convective systems in central equatorial Africa. Int. J. Climatol. ***41***, 469–482.
39. Dommo, A., Philippon, N., Vondou, D.A., et al. (2018). The June-September low cloud cover in western central Africa: mean spatial distribution and diurnal evolution, and associated atmospheric dynamics. J. Clim. ***31***, 9585–9603.
40. Philippon, N., Cornu, G., Monteil, L., et al. (2019). The light-deficient climates of western Central African evergreen forests. Environ. Res. Lett. ***14***, 034007.
41. Kikuzawa, K. (1991). A cost-benefit analysis of leaf habit and leaf longevity of trees and their geographical pattern. Am. Nat. ***138***, 1250–1263.
42. Kikuzawa, K. (1995). Leaf phenology as an optimal strategy for carbon gain in plants. Can. J. Bot. ***73***, 158–163.
43. Vico, G., Thompson, S.E., Manzoni, S., et al. (2015). Climatic, ecophysiological, and phenological controls on plant ecohydrological strategies in seasonally dry ecosystems. Ecohydrol ***8***, 660–681.
44. Brodribb, T.J., Holbrook, N.M., and Gutierrez, M.V. (2002). Hydraulic and photosynthetic co-ordination in seasonally dry tropical forest trees. Plant Cell Environ ***25***, 1435–1444.
45. Lee, J.E., and Boyce, K. (2010). The impact of hydraulic capacity on water and carbon cycles in tropical South America. J. Geophys. Res. ***115***, D23123.
46. Lopes, A.P., Nelson, B.W., Wu, J., et al. (2016). Leaf flush drives dry season green-up of the Central Amazon. Remote Sens. Environ. ***182***, 90–98.
47. Reichstein, M., Tenhunen, J.D., Roupsard, O., et al. (2002). Severe drought effects on ecosystem CO_2 and H_2O fluxes at three Mediterranean evergreen sites: revision of current hypotheses? Glob. Change Biol ***8***, 999–1017.
48. Shirke, P.A., and Pathre, U.V. (2004). Influence of leaf-to-air vapour pressure deficit (VPD) on the biochemistry and physiology of photosynthesis in *Prosopis juliflora*. J. Exp. Bot. ***55***, 2111–2120.
49. McAdam, S.A.M., and Brodribb, T.J. (2016). Linking turgor with ABA biosynthesis: implications for stomatal responses to vapor pressure deficit across land plants. Plant Physiol. ***171***, 2008–2016.
50. Nepstad, D.C., Moutinho, P., Dias-Filho, M.B., et al. (2002). The effects of partial throughfall exclusion on canopy processes, aboveground production, and biogeochemistry of an Amazon forest. J. Geophys. Res-atmos. ***107***. https://doi.org/10.1029/2001JD000360.
51. Brodribb, T.J., Powers, J., Cochard, H., et al. (2020). Hanging by a thread? Forests and drought. Science ***368***, 261–266.
52. Rowland, L., da Costa, A.C.L., Galbraith, D.R., et al. (2015). Death from drought in tropical forests is triggered by hydraulics not carbon starvation. Nature ***528***, 119–122.
53. Xu, X., Medvigy, D., Powers, J.S., et al. (2016). Diversity in plant hydraulic traits explains seasonal and inter-annual variations of vegetation dynamics in seasonally dry tropical forests. New Phytol. ***212***, 80–95.
54. Graham, E.A., Mulkey, S.S., Kitajima, K., et al. (2003). Cloud cover limits net CO_2 uptake and growth of a rainforest tree during tropical rainy seasons. Proc. Natl. Acad. Sci. USA ***100***, 572–576.
55. Zalamea, M., and Gonzalez, G. (2008). Leaffall phenology in a subtropical wet forest in Puerto Rico: from species to community patterns. Biotropica ***40***, 295–304.
56. Poorter, L., Rozendaal, D.M.A., Bongers, F., et al. (2019). Wet and dry tropical forests show opposite successional pathways in wood density but converge over time. Nat. Ecol. Evol. ***3***, 928–934.
57. Martinez-Yrizar, A., and Sarukhan, J. (1990). Litterfall patterns in a tropical deciduous forest in Mexico over a five-year period. J. Trop. Ecol. ***6***, 433–444.
58. Angulo-Sandoval, P., and Aide, T.M. (2000). Leaf phenology and leaf damage of saplings in the Luquillo Experimental Forest, Puerto Rico. Biotropica ***32***, 415–422.
59. Descheemaeker, K., Muys, B., Nyssen, J., et al. (2006). Litter production and organic matter accumulation in exclosures of the Tigary highlands, Ethiopia. For. Ecol. Manage. ***233***, 21–35.
60. Pearse, I.S., Koenig, W.D., and Kelly, D. (2016). Mechanisms of mast seeding: resources, weather, cues, and selection. New Phytol. ***212***, 546–562.
61. Detto, M., Wright, S.J., Calderón, O., et al. (2018). Resource acquisition and reproductive strategies of tropical forest in response to the El Niño-Southern Oscillation. Nat. Commun. ***9***, 913.
62. Trugman, A.T., Anderegg, L.D.L., Wolfe, B.T., et al. (2019). Climate and plant trait strategies determine tree carbon allocation to leaves and mediate future forest productivity. Glob. Change Biol ***25***, 3395–3405.
63. Huete, A.R., Didan, K., Shimabukuro, Y.E., et al. (2006). Amazon rainforests green-up with sunlight in dry season. Geophys. Res. Lett. ***33***, L06405.
64. Myneni, R.B., Yang, W., Nemani, R.R., et al. (2007). Large seasonal swings in leaf area of Amazon rainforests. Proc. Natl. Acad. Sci. USA ***104***, 4820–4823.
65. Wu, J., Kobayashi, H., Stark, S.C., et al. (2018). Biological processes dominate seasonality of remotely sensed canopy greenness in an Amazon evergreen forest. New Phytol. ***217***, 1507–1520.
66. Du, J., Kimball, J.S., Jones, L.A., et al. (2017). A global satellite environmental data record derived from AMSR-E and AMSR2 microwave Earth observations. Earth Syst. Sci. Data ***9***, 791.
67. Fan, Y., Miguez-Macho, G., Jobbágy, E.G., et al. (2017). Hydrologic regulation of plant rooting depth. Proc. Natl. Acad. Sci. USA ***114***, 10572–10577.
68. Chen, X., Ciais, P., Maignan, F., et al. (2021). Vapor pressure deficits and sunlight explain seasonality of leaf phenology and photosynthesis across Amazonian evergreen broadleaved forest. Glob. Biogeochem. Cy. ***35***. https://doi.org/10.1029/2020GB006893.
69. Wright, S.J. (1996). Phenological responses to seasonality in tropical forest plants. In Tropical Forest Plant Ecophysiology, S.S. Mulkey, R.L. Chazdon, and A.P. Smith, eds. (Chapman and Hall), pp. 440–460.

ACKNOWLEDGMENTS

A special thanks to the anonymous reviewers and Dr. Jin Wu from the Hong Kong University for their constructive suggestions. This study was supported by the Guangdong Major Project of Basic and Applied Basic Research (grant number 2020B0301030004), the National Natural Science Foundation of China (grant numbers 31971458, 41971275), the Special high-level plan project of Guangdong Province (grant number 2016TQ03Z354), Innovation Group Project of Southern Marine Science and Engineering Guangdong Laboratory (Zhuhai) (grant number 311021009), the Guangdong Basic and Applied Basic Research Foundation (grant number 2020A151501091), and GDAS Special Project of Science and Technology Development (grant number 2020GDASYL-20200102002).

AUTHOR CONTRIBUTIONS

X.C., P.C., Y.S., and S.J.W. designed the study and wrote the paper. X.Y., J.W., X.C., F.G., Y.S., Y.D., and L.L. collected and analyzed the data and drew the figures. All authors contributed to editing the text and discussed the scientific questions.

DECLARATION OF INTERESTS

The authors declare no competing interests.

LEAD CONTACT WEBSITE

https://chenxiuzhi.wordpress.com.

SUPPLEMENTAL INFORMATION

Supplemental information can be found online at https://doi.org/10.1016/j.xinn.2021.100154.